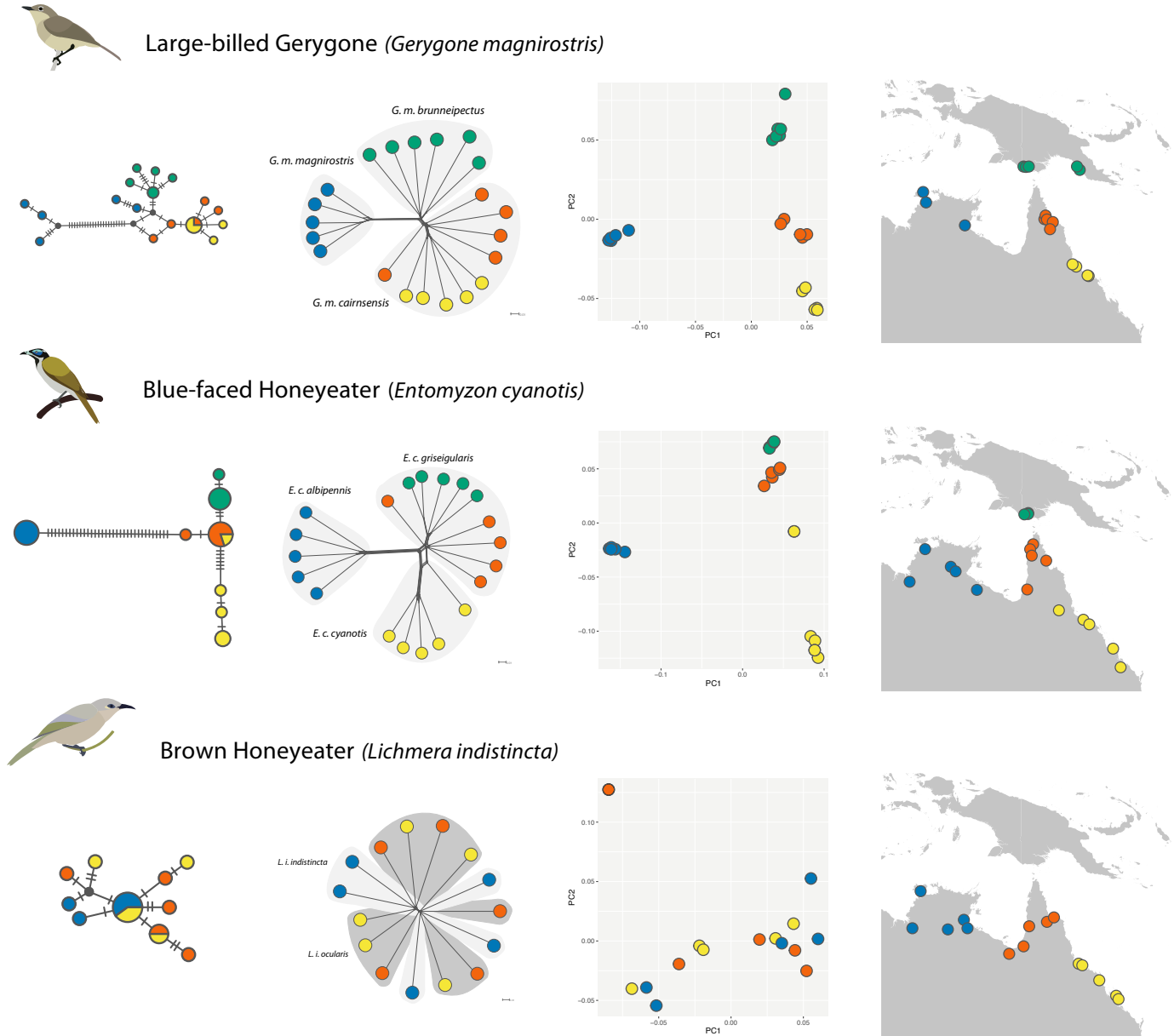


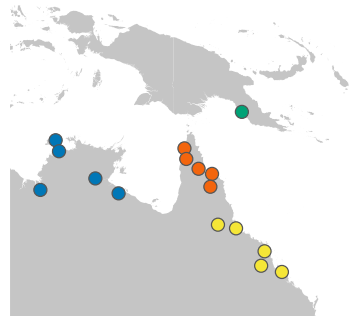
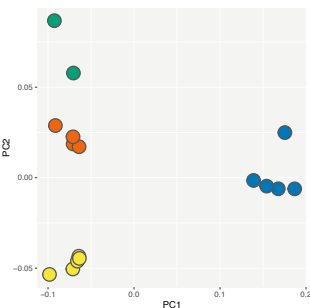
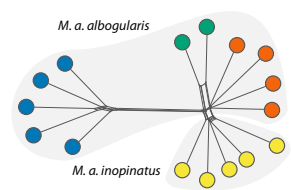
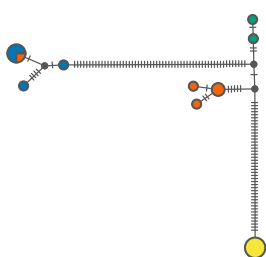
SUPPLEMENTARY FIGURES

Figure S1. Population structure of each species represented by ND2 haplotype networks, ddRAD sampling networks, and principal coordinates analyses next to their geographic sampling locations.

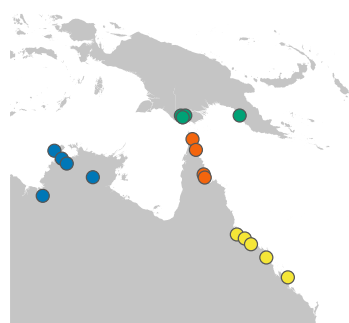
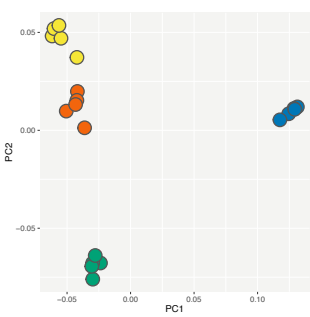
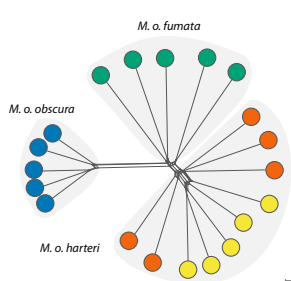
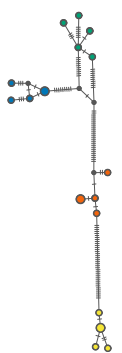




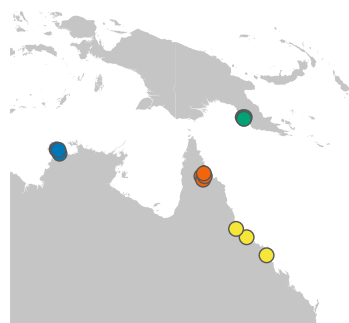
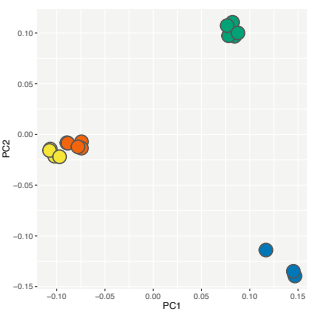
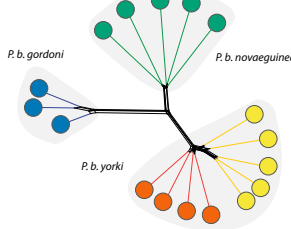
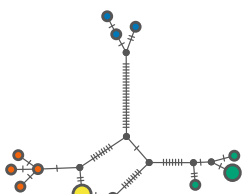
White-throated Honeyeater (*Melithreptus albogularis*)



Dusky Myzomela (*Myzomela obscura*)

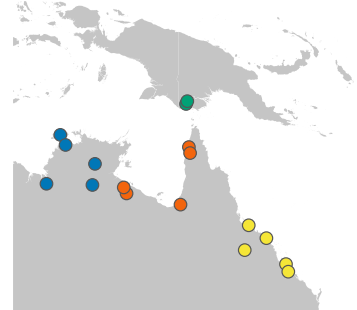
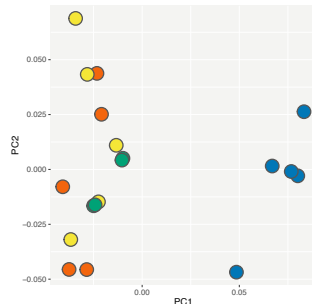
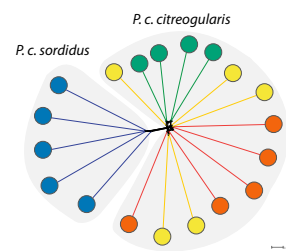
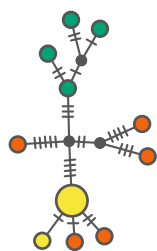


Helmeted Friarbird (*Philemon buceroides*)





Little Friarbird (*Philemon citreogularis*)



Yellow-tinted x Fuscous Honeyeater (*Ptilotula flavescens x fuscus*)

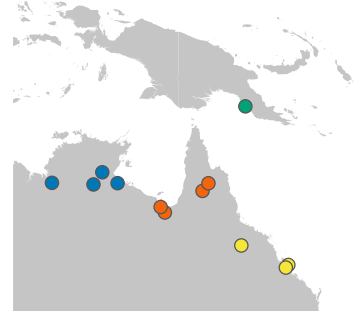
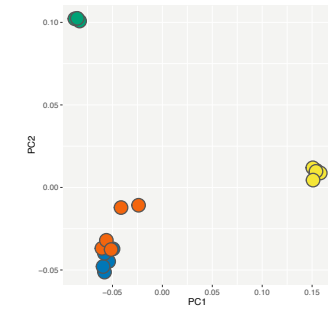
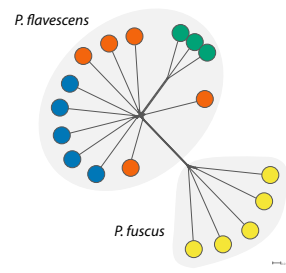
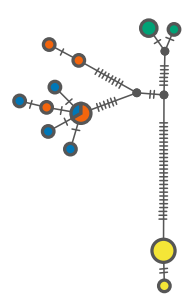


Figure S2. Graphical illustrations representing the models describing the accumulation of incompatibilities. The x-axis represents the divergence and y-axis represents the number incompatibilities between populations.

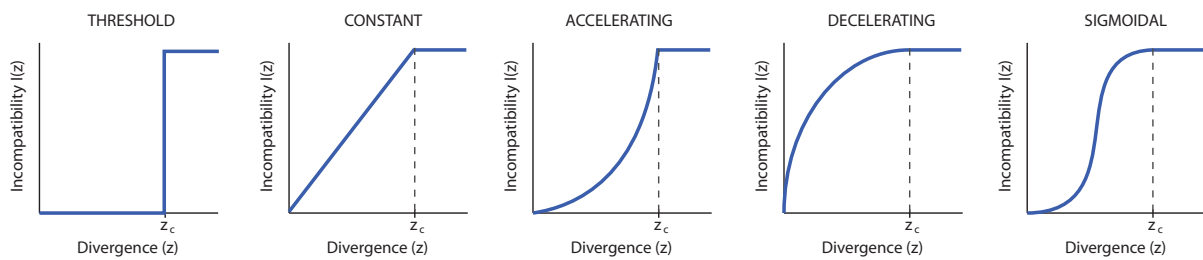
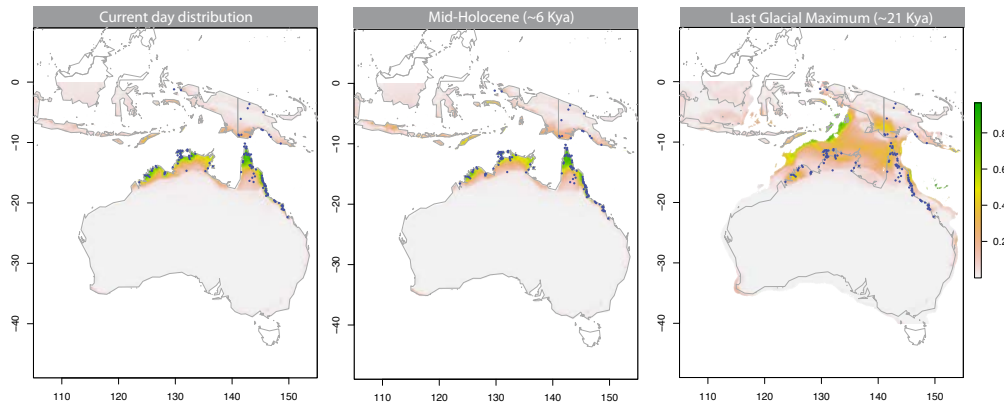


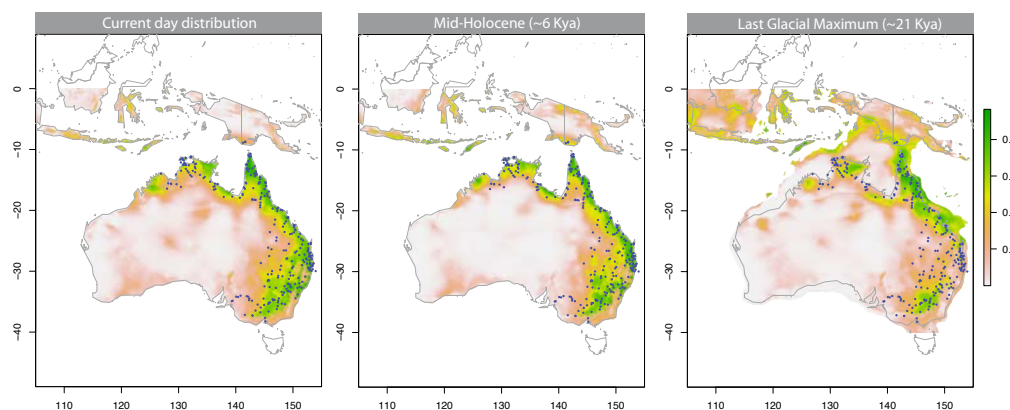
Figure S3. Species distribution models using MAXENT and the points used for the prediction.



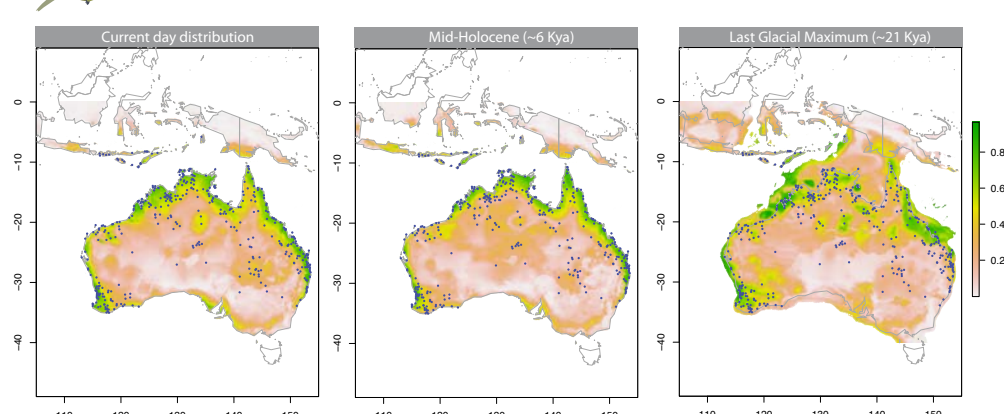
Large-billed Gerygone (*Gerygone magnirostris*)



Blue-faced Honeyeater (*Entomyzon cyanotis*)

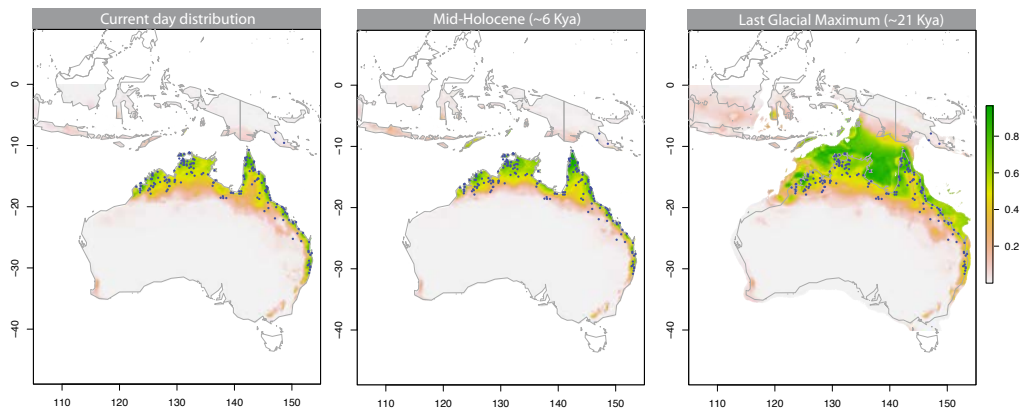


Brown Honeyeater (*Lichenmera indistincta*)

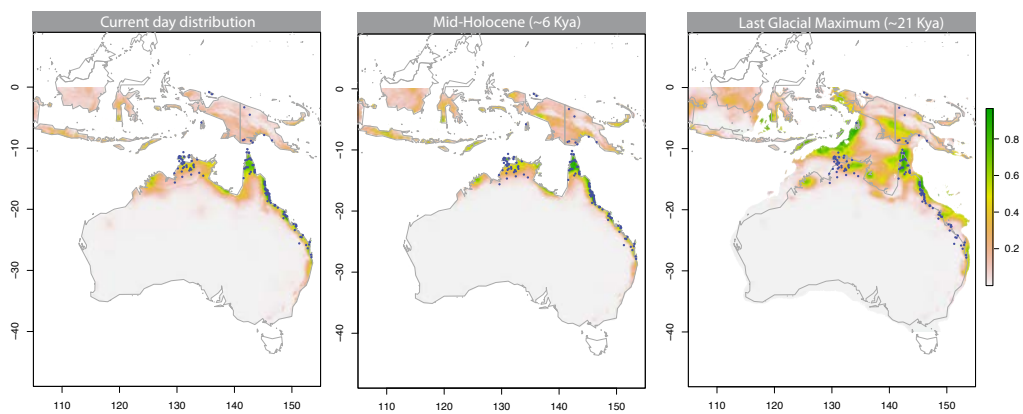




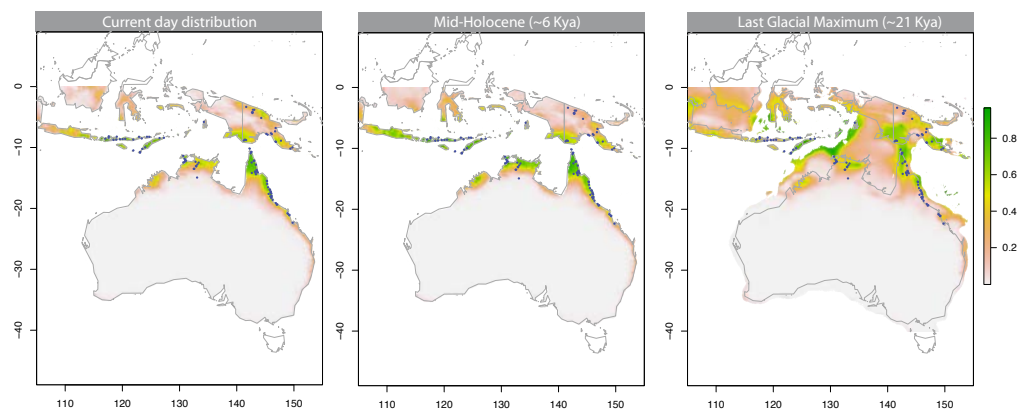
White-throated Honeyeater (*Melithreptus albogularis*)



Dusky Myzomela (*Myzomela obscura*)

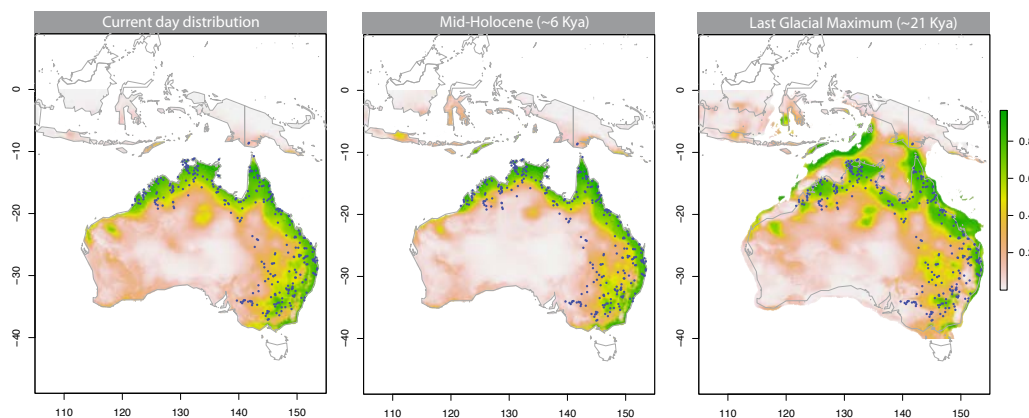


Helmeted Friarbird (*Philemon buceroides*)





Little Friarbird (*Philemon citreogularis*)



Yellow-tinted x Fuscous Honeyeater (*Ptilotula flavescens x fuscous*)

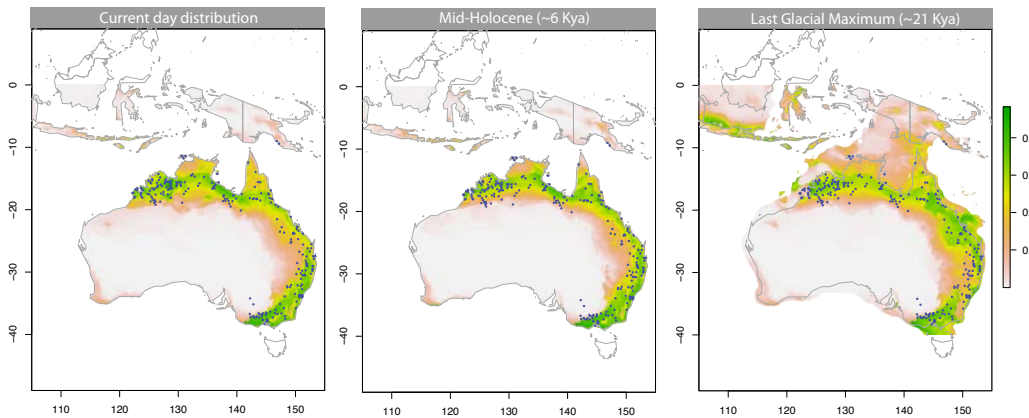


Figure S4. Plots of the correlations of various divergence measures between the autosomes and the Z chromosome.

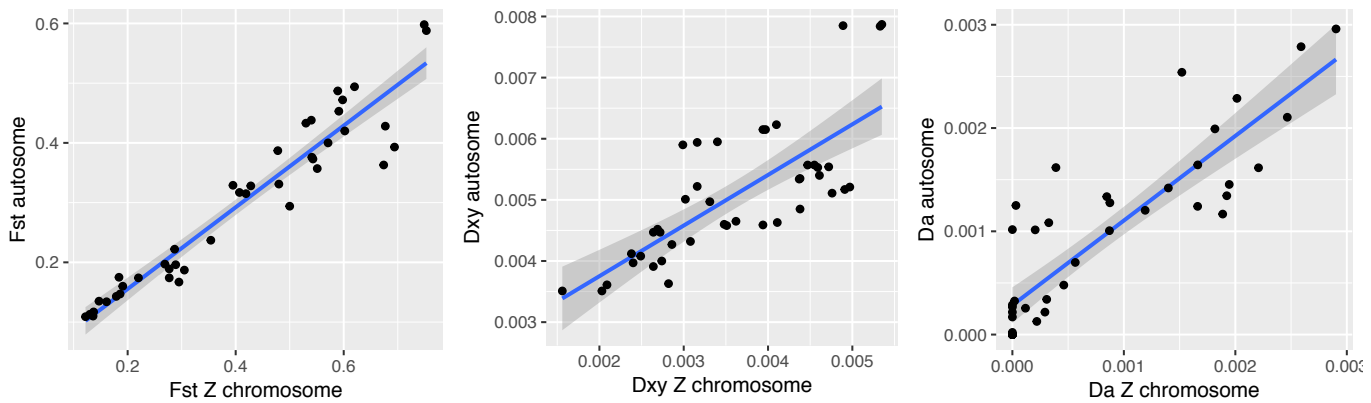


Figure S5. ND2 p-distances and D_{XY} plotted against F_{ST} . The plots show a small range of ND2 divergence levels where probability of migration quickly transitions between high to low. A few outliers may represent systems where mitochondrial divergence accumulated in periods of allopatry and were maintained after secondary contact while there was gene flow in the nuclear genome.

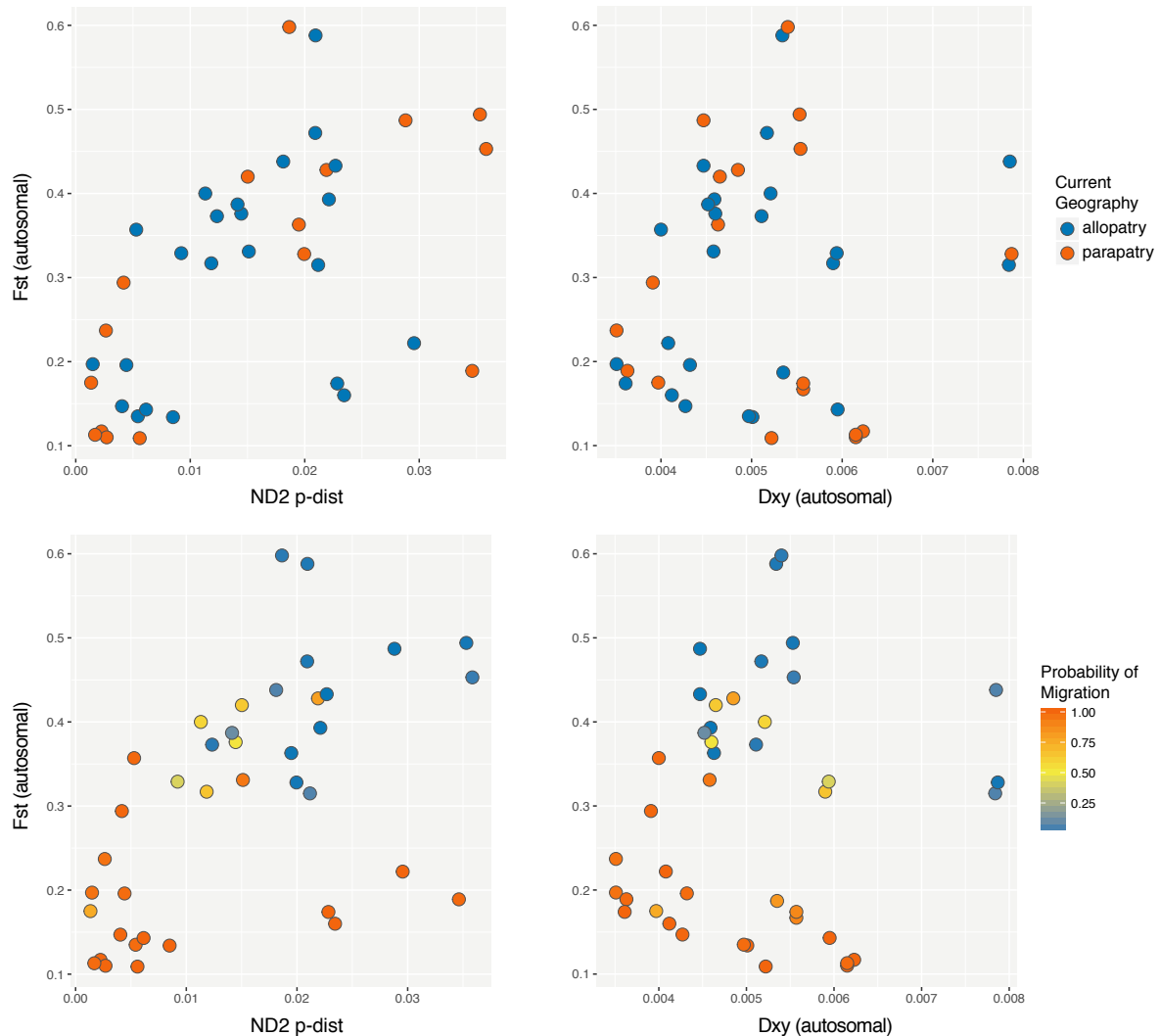


Figure S6. Plot showing the increasing difference between autosomal and Z chromosome divergence through increasing divergence. The points are colored by probability of migration with red having higher likelihood of gene flow and blue having a low likelihood of gene flow. Low probability of migration tends to have a larger difference between autosomal and Z chromosome divergence.

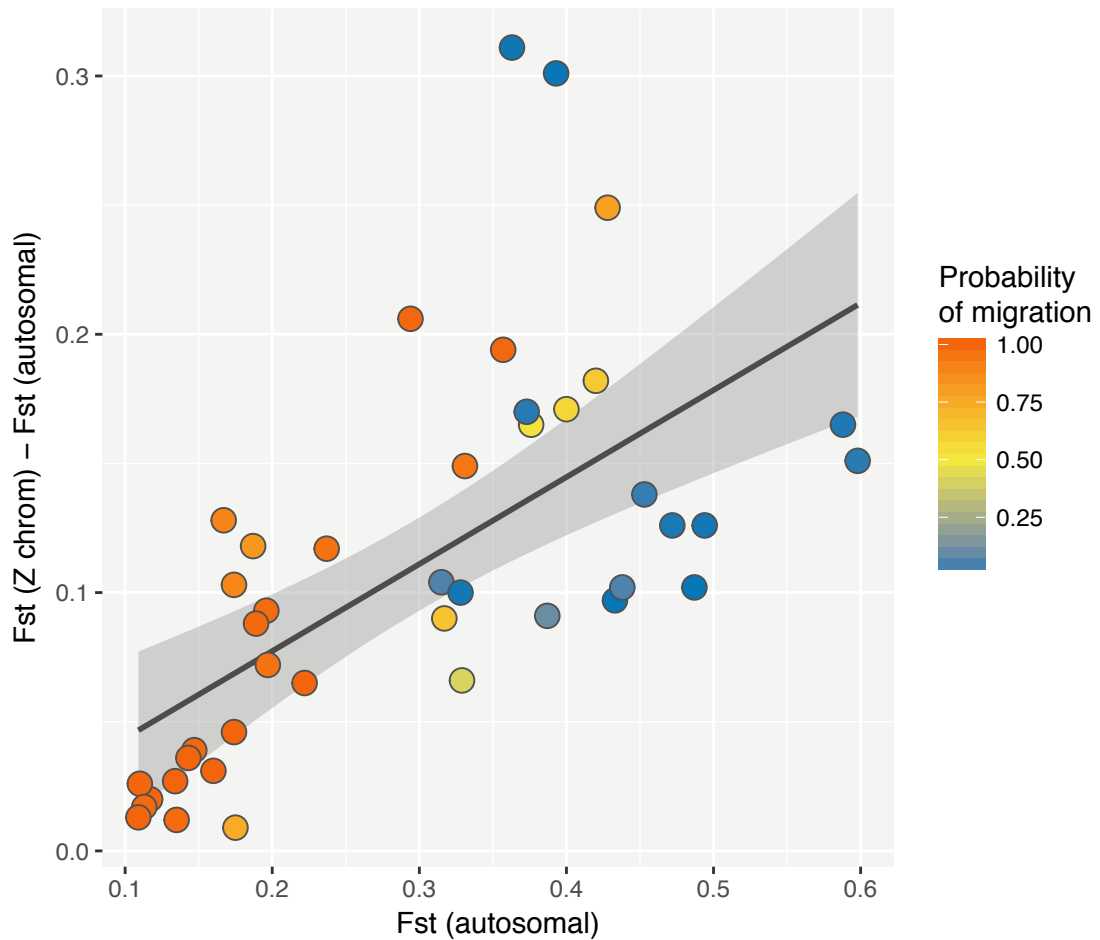
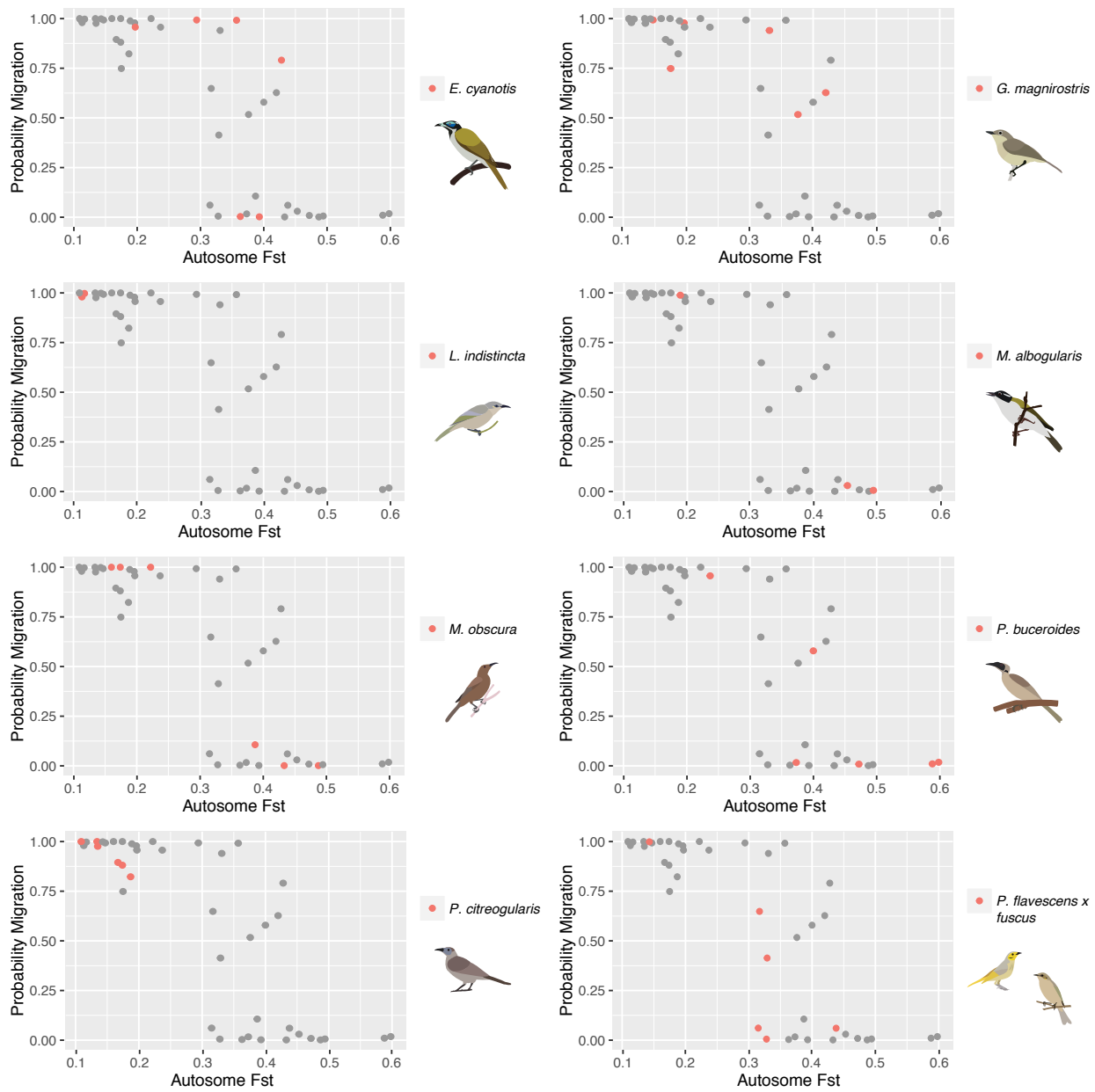


Figure S7. Plots highlighting species-specific points in the trajectory of decreasing probability of migration with increasing F_{ST} .



S8. Plots of the decreasing likelihood of gene flow with 3 measures of genetic divergence (F_{ST} , D_{XY} , and D_A) for autosomal and Z chromosome. Likelihood of gene flow was also plotted against ND2 p-distance.

